Am J Transl Res 2019;11(3):1446-1459
www.ajtr.org /ISSN:1943-8141/AJTR0087298

Original Article

Low-dose tubacin promotes BMSCs proliferation and morphological changes through the ERK pathway

Jia-Qiang Liang[1], Fang Lu[1,4*], Bin Gan[5*], Yu-Ying Wen[1], Jin Chen[1], Huai-Gao Wang[1], Yang Yang[1], Xin-Sheng Peng[2,3], Yan-Fang Zhou[1]

[1]Department of Pathophysiology, [2]Biomedical Innovation Center, [3]Institute of Marine Medicine, Guangdong Medical University, Dongguan 523808, China; [4]Department of Pathology, Guangdong Second Provincial General Hospital, Guangzhou 510317, China; [5]The Third Affiliated Hospital of Guangdong Medical University, Fo Shan 528000, Guangdong, China. [*]Equal contributors.

Received October 25, 2018; Accepted January 9, 2019; Epub March 15, 2019; Published March 30, 2019

Abstract: Histone deacetylase 6 (HDAC6) plays critical roles in many cellular processes related to cancer, but its epigenetic regulation in bone marrow stromal stem cells (BMSCs) remains unexplored. This study investigated the beneficial effects of Tubulin Acetylation Inducer (tubacin), a novel specific HDAC6 inhibitor, on the proliferation and migration of BMSCs. A low concentration of tubacin promoted BMSC commitment and enhanced proliferation of BMSCs. Atomic force microscopy results showed that tubacin induced morphological changes and enhanced the mechanical properties of BMSCs. Furthermore, low tubacin concentrations significantly upregulated protein expression of acetylated α-tubulin, VCAM-1, and ICAM-1, which could be suppressed by an ERK inhibitor. Protein chip analysis showed that there were significant changes in the expression levels of 49 cytokines after tubacin treatment, which participate in inflammatory responses and cell activation, proliferation, and differentiation. Our findings suggest that the protective effects of tubacin on BMSCs involve HDAC6 inhibition by activating the ERK pathway.

Keywords: Histone deacetylase 6, tubacin, bone marrow stromal stem cells (BMSCs), proliferation, migration

Introduction

Bone marrow stromal stem cells (BMSCs) are a class of multipotent adult stem cells with characteristics of self-proliferation and high plasticity. Studies on the pluripotency of BMSCs have laid a solid foundation for their clinical application in regenerative medicine [1]. BMSCs differentiate into mesoderm-derived tissues *in vitro* and *in vivo* and secrete a range of trophic factors which can initiate the regeneration of many tissues. Studies have shown that BMSCs selectively home to injury sites and exhibit the potential to improve cellular function.

However, clinical application of cell therapy is hampered by the fact that BMSCs are prone to apoptosis in ischemic and anoxic environments [2-5]. Furthermore, when BMSCs are applied to an entire organism, only a few of the injected BMSCs reach the ischemic tissue, as most of the cells are trapped in the lung. The ability of stem cells to continually proliferate and migrate to injury sites may be beneficial in regenerative medicine.

Histone deacetylase 6 (HDAC6) is a member of the HDAC enzyme family. These proteins regulate acetylation of histone proteins and non-histone proteins, leading to chromatin condensation and repression of gene transcription. HDAC6 is a known regulator of cell motility via control of the tubulin, cortactin, and actin networks and promotes endothelial cell migration as well as angiogenesis [6, 7]. Indeed, overexpression of HDAC6 promotes tumorigenesis, enhances invasive metastatic features, and improves tumor survival. However, the function of HDAC6 in stem cell proliferation and migration remains largely unknown.

A previous study reported that HDAC6 contributes to stem cell commitment and influences stem cell differentiation. HDAC6 is a critical regulator of mitochondrial function in BMSCs, and modulation of HDAC6 activity could be a

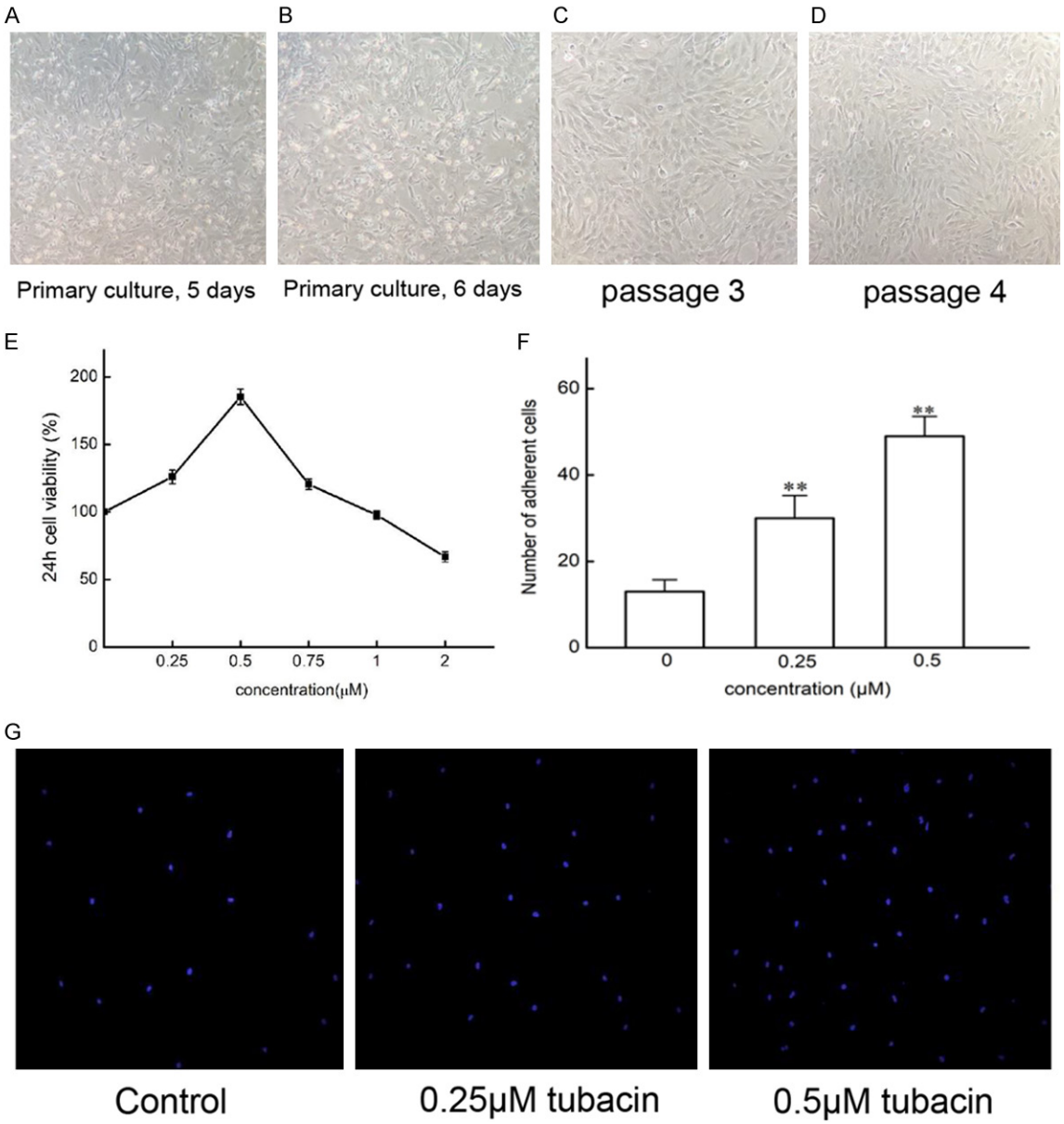

Figure 1. BMSC morphology at different time points and the effects of different concentrations of tubacin on BMSC cell viability and adhesion. A. Primary culture of BMSCs, 40 ×, 5 days. B. Primary culture of BMSCs, 40 ×, 6 days. C. Passage 3 BMSCs, 40 ×. D. Passage 4 BMSCs, 40 ×. E. Cell viability after treatment with different concentrations of tubacin (24 h). G. Representative images of the cell adhesion experiments. BMSCs were divided into three groups: untreated control cells, 0.25 μM tubacin group, and 0.5 μM tubacin group. The adhesion experiment was performed three times. F. Quantitative analyses of the number of adherent cells. Data are presented as mean ± SD. $^{**}P < 0.01$ compared with the control group.

novel approach to improve BMSC-based therapies [8]. Downregulation of HDAC6 stimulates endogenous neural stem cell proliferation and angiogenesis [9-11], reduces the area of cerebral ischemia [12-14], increases the secretion of brain-derived neurotrophic factor and vascular endothelial growth factor [15-17], and promotes the repair of damaged nerves in cerebral ischemia.

In the present study, we report another key role of HDAC6 in stem cell survival. Low concentrations of the HDAC6 inhibitor tubacin promoted BMSC commitment and enhanced the proliferation of BMSCs to a higher extent than high concentrations. Mechanically, downregulation of HDAC6 was demonstrated to promote acetylation of α-tubulin, VCAM-1, and ICAM-1, which could be suppressed by the ERK inhibitor

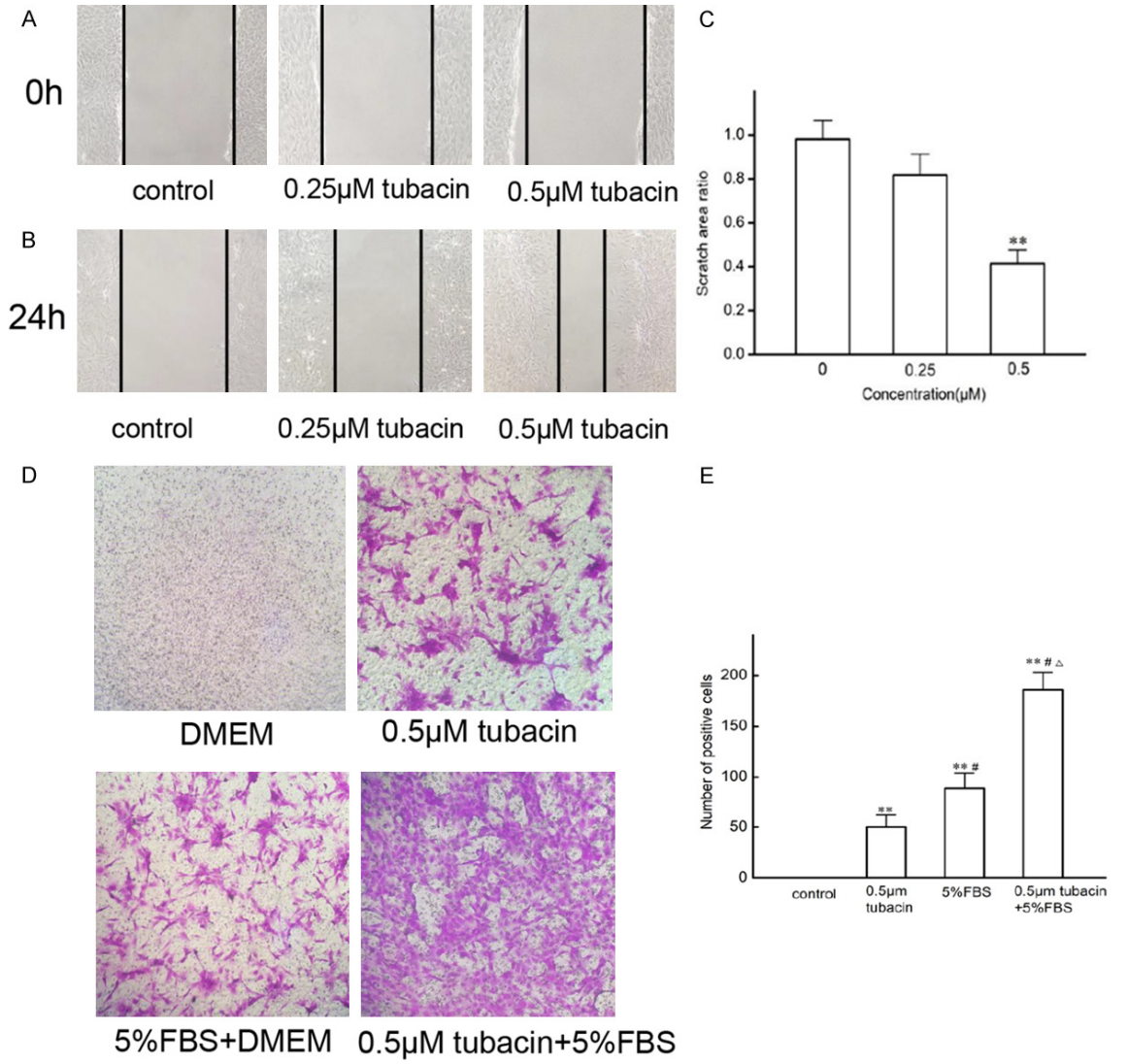

Figure 2. Effects of different concentrations of tubacin on BMSC migration. BMSCs were divided into three groups: untreated control cells, 0.25 μM tubacin group, and 0.5 μM tubacin group. A. Scratch area of each group at 0 h. B. Scratch area of each group at 24 h. The images were analyzed with ImageJ software; the corresponding scratch area was analyzed, and the ratio of the scratch area between 24 h and 0 h was calculated. C. 24 h/0 h scratch area chart. Data are presented as mean ± SD. Comparisons were performed by one-way analysis of variance (ANOVA) among groups or by Student's t test between two groups. $^{**}P < 0.01$ compared with the control group. D. Cells that migrated from the upper chamber to the lower chamber surface were fixed and stained with crystal violet. E. The experiment was repeated three times and the migrating cells were counted for statistical analysis. Data are presented as mean ± SD. A student's t test was performed to evaluate the difference. $^{**}P < 0.01$ compared with the control group; $\#P < 0.01$ compared with the 0.5 μM tubacin group; $\Delta P < 0.01$ compared with the 5% FBS group.

U0126. The results indicate that modulation of HDAC6 activity could play a key role in BMSC transplantation.

Materials and methods

Materials

DMEM/F12 liquid medium, fetal bovine serum (FBS), and trypsin were purchased from Gibco (USA). Tubacin was purchased from Sigma (USA). Dimethyl sulfoxide (DMSO) was purchased from Solarbio (Beijing, China). MTT was purchased from Huamei Bio-Engineering (Beijing, China). U0126 was purchased from Cell Signaling Technology (USA). The following primary antibodies were purchased from Sigma (USA): anti-HDAC6 (1:1000) and anti-α-tubulin (1:1000). The following primary antibodies were purchased from Cell Signaling Technology

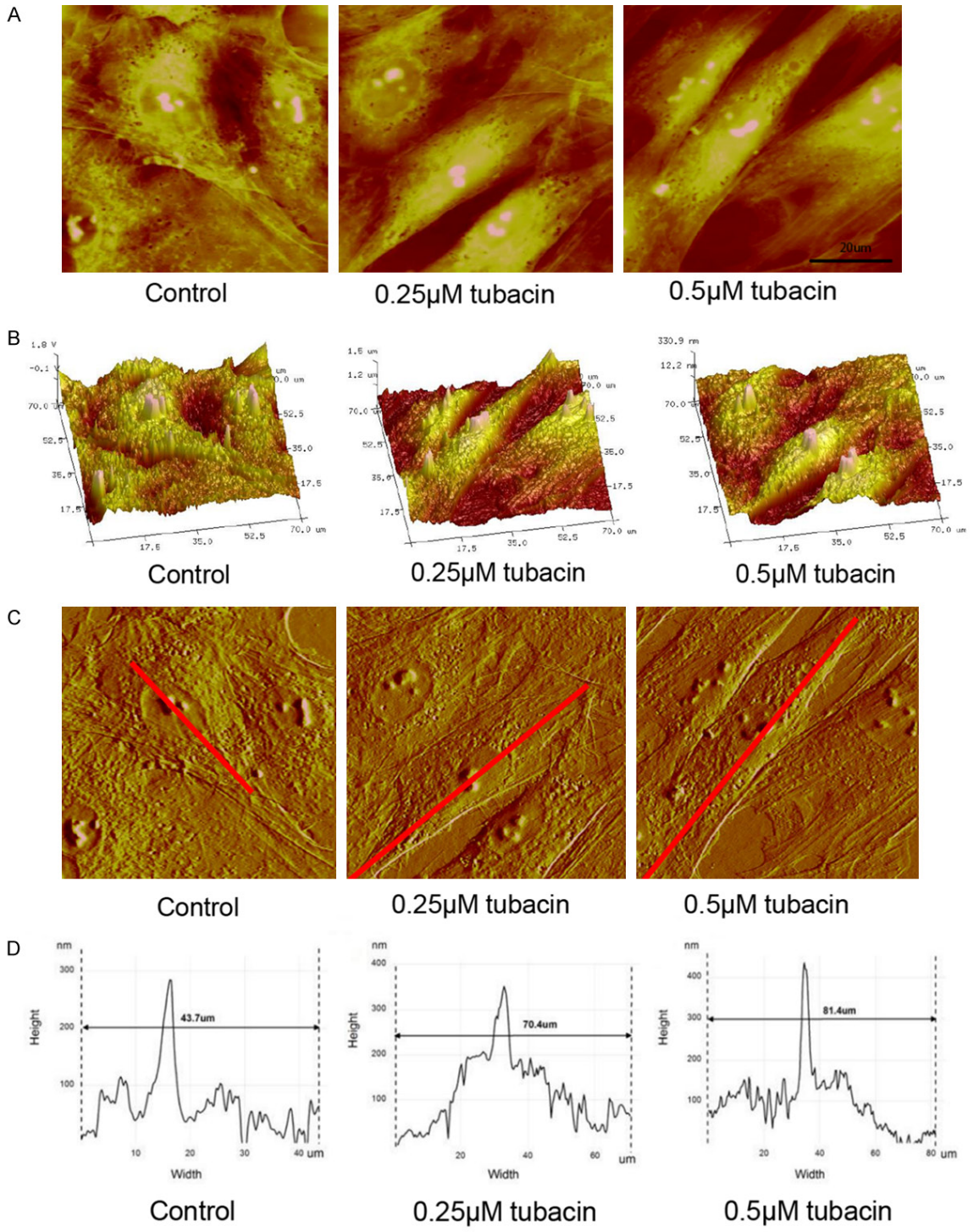

Figure 3. 2D morphology, 3D topography, and height of BMSCs. BMSCs were divided into three groups: untreated control cells, 0.25 μM tubacin group, and 0.5 μM tubacin group. A. Two-dimensional images of BMSCs. B. Three-dimensional images of BMSCs. C. The red line indicates the long diameter of BMSCs. Scale bar: 20 μm. D. Observed and measured results of the long diameter and height.

(USA): rabbit anti-mouse beta-actin monoclonal antibody (1:1000), anti-ICAM-1 (1:1000), anti-VCAM-1 (1:1000), anti-ERK (1:1000), anti-p-ERK (1:1000), anti-Akt (pan) (1:1000) and anti-Phospho-Akt (Ser473) (1:1000). Goat anti-rabbit secondary antibodies labeled with horse-

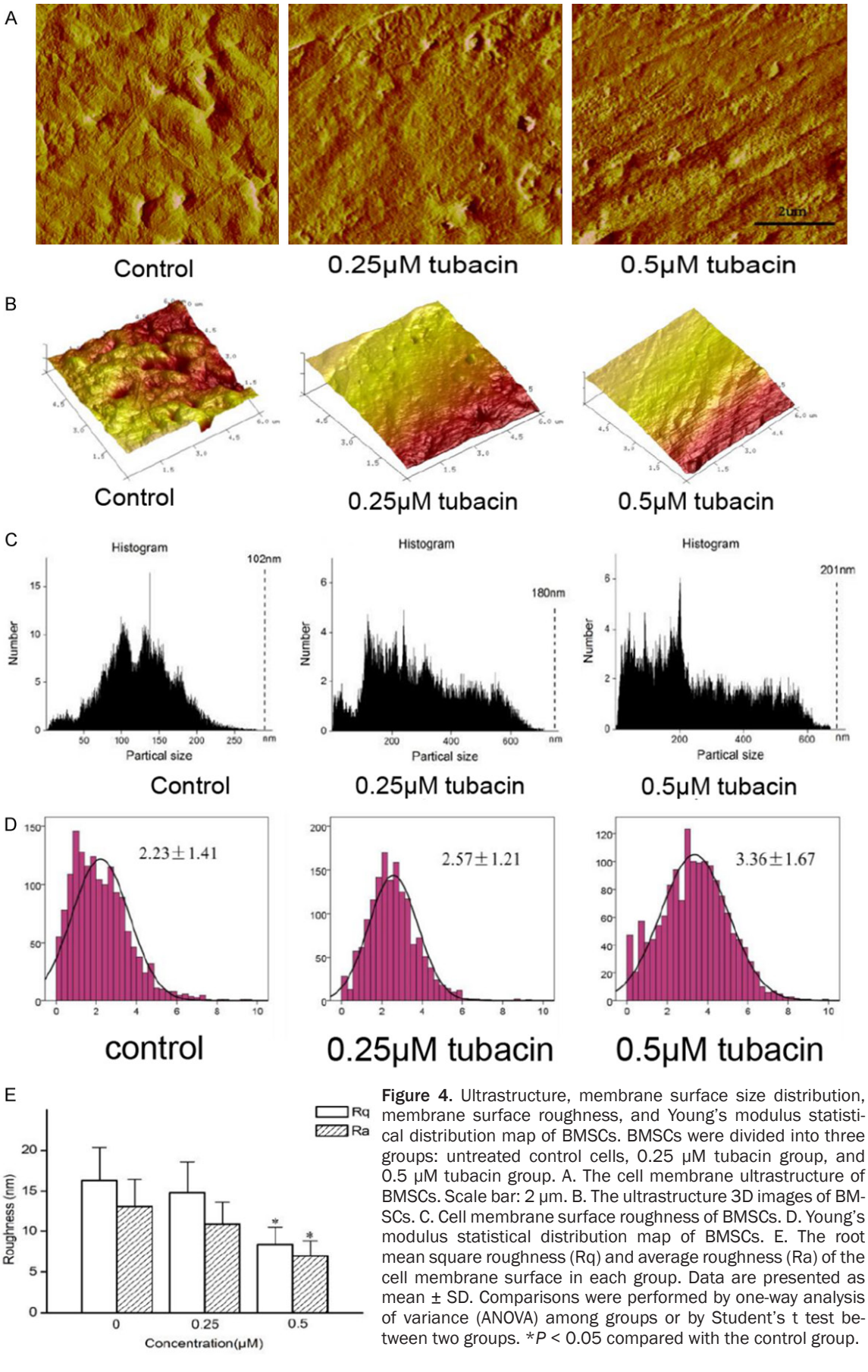

Figure 4. Ultrastructure, membrane surface size distribution, membrane surface roughness, and Young's modulus statistical distribution map of BMSCs. BMSCs were divided into three groups: untreated control cells, 0.25 μM tubacin group, and 0.5 μM tubacin group. A. The cell membrane ultrastructure of BMSCs. Scale bar: 2 μm. B. The ultrastructure 3D images of BMSCs. C. Cell membrane surface roughness of BMSCs. D. Young's modulus statistical distribution map of BMSCs. E. The root mean square roughness (Rq) and average roughness (Ra) of the cell membrane surface in each group. Data are presented as mean ± SD. Comparisons were performed by one-way analysis of variance (ANOVA) among groups or by Student's t test between two groups. *$P < 0.05$ compared with the control group.

Table 1. The root mean square roughness (Rq) and average roughness (Ra) of the membrane surface of BMSCs

Group	Rq (nm)	Ra (nm)
Control	16.28 ± 4.10	13.12 ± 3.31
0.25 μM tubacin	14.80 ± 3.83	10.89 ± 2.80
0.5 μM tubacin	8.34 ± 2.20*	6.94 ± 1.89*

Data are presented as mean ± SD. Comparisons were performed by one-way analysis of variance (ANOVA) among groups or by Student's t test between two groups. *P < 0.05 compared with the control group.

radish peroxidase were also purchased from Cell Signaling Technology (USA). The BCA Protein Assay Kit and Hoechst 33258 stain were purchased from Biyuntian Biotechnology Research Institute (Guangzhou, China). Protease Inhibitor Cocktail was purchased from Roche (Germany). All of the other chemicals and reagents were of analytical grade.

Isolation and culture of primary BMSCs

All of the animal operations were performed in accordance with NIH guidelines and ethical principles for the care and use of laboratory animals and were approved by the experimental animal center of Southern Medical University. All of the experimental animals were treated humanely. Briefly, an incision was made in the tibias and femurs of male Sprague-Dawley rats, and the cavernous bone marrow was extracted under aseptic conditions. Subsequently, rat BMSCs were isolated from the bone marrow by centrifugation at 1000 rpm for 10 min. The isolated BMSCs were cultured in DMEM supplemented with FBS at 37°C in a 5% CO_2 incubator. Cells from passages 2-4 were used for the following experiments.

Proliferation assay

The cells were inoculated into 96-well plates at 2000 cells per well. After the cells adhered to the plate, the medium was aspirated, the cells were pretreated with 10 μM U0126 for 2 h, and 200 μl medium containing different concentrations of tubacin was added to each group. The same volume of serum-free medium was added as a negative control group and incubated for 24 h. MTT solution (5 g/l) was added to each well and cells were cultured for an additional 4 h. The supernatant was aspirated, 200 μl DMSO was added to each well, the plates were shaken for 10 min to dissolve the crystals, and the OD value of each well was measured on a microplate reader at a wavelength of 490 nm. The cell survival rate was calculated as follows: cell survival rate (%) = [(As-Ab)/(Ac-Ab)] × 100%, where As is the OD value of the experimental wells, Ac is the OD value of the control wells, and Ab is the blank OD value. The results are expressed as the means ± SD (n = 5). The data are presented in a graph, with the tubacin concentration on the horizontal axis and the cell survival rate on the vertical axis.

AFM morphology imaging and membrane ultrastructure analysis

BMSCs were exposed to air and images were captured at 0.8 Hz scan speed. More than three cells were measured in each group. All of the topographical images were evaluated by Nanoscope 8.14 analysis software. The cell surface root mean square roughness (Rq) and average roughness (Ra) were calculated for different areas of 2 × 2 μm^2.

Wound healing assay

The BMSCs were plated at 2 × 10^5 cells/ml in 24-well plates in DMEM/F12 medium with 10% FBS and with different tubacin concentrations. At 100% confluency, a linear wound was simulated by scratching. Cells were washed twice with PBS and incubated in fresh medium for 24 h. Cells were then visualized by microscopy and the healed area was measured.

Transwell invasion and migration assay

For the migration assay, the BMSCs were plated at 2 × 10^4 cells/ml in an 8-μm Transwell chamber containing polycarbonate filters. To each well, 600 μl DMEM/F12 with different concentrations of tubacin was added. The cells were cultured at 37°C with 5% CO_2. After 24 h, the transwell chamber was removed, and the cells were washed twice with PBS, fixed with methanol at room temperature for 30 min, washed twice with PBS, stained with 0.1% crystal violet for 15 minutes, and again washed twice with PBS. The cells on the surface of the chamber were gently wiped off with a cotton ball, and the cells were observed under a microscope (magnification: × 40). Ten fields were randomly selected to record the number of stained cells in each group.

Adhesion experiment

The BMSCs were pretreated with different concentrations of tubacin for 24 h. The cells were pretreated with 10 μM U0126 for 2 h. The

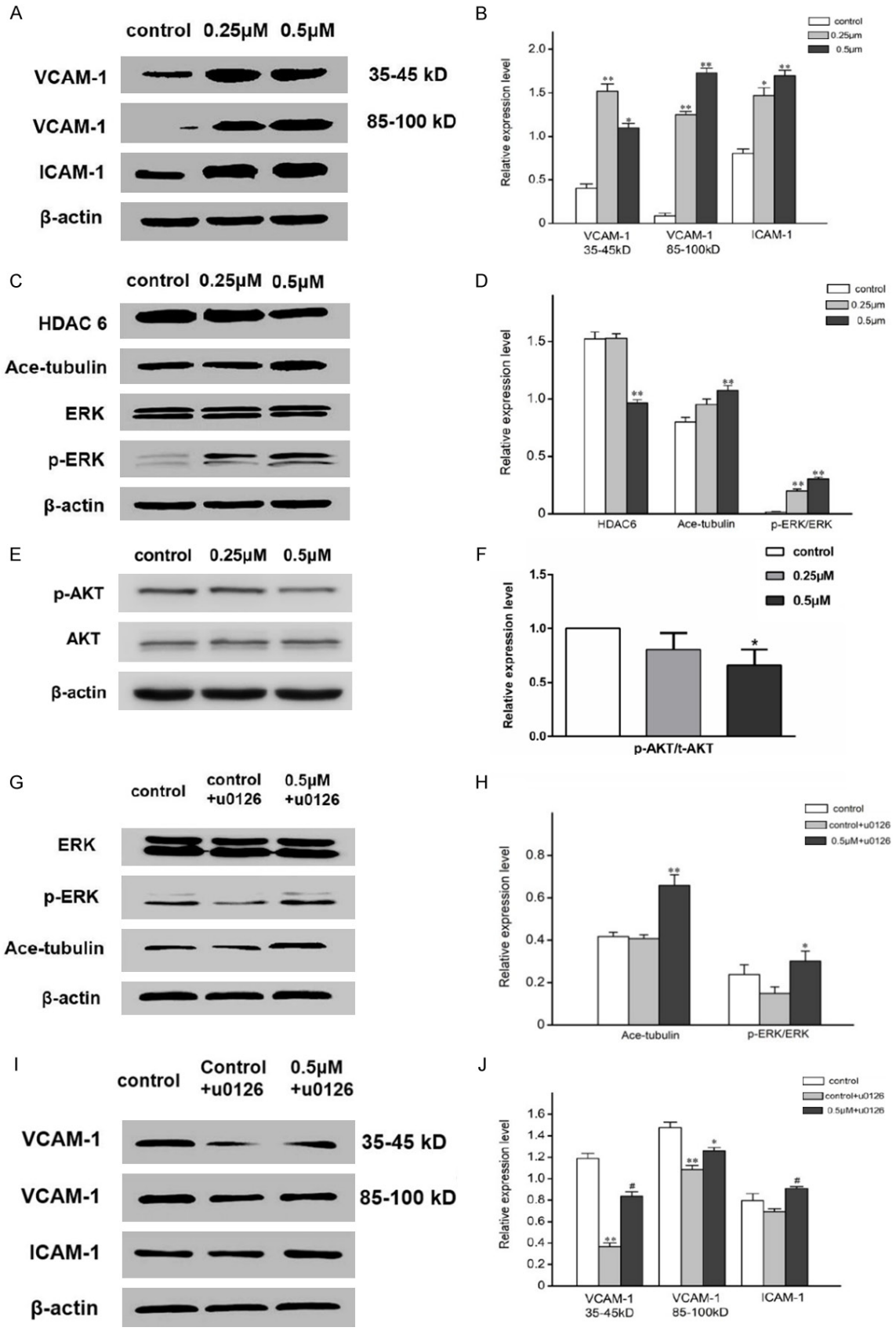
A
control 0.25μM 0.5μM
VCAM-1
35-45 kD
VCAM-1
85-100 kD
ICAM-1
β-actin
B
control
0.25μm
0.5μm
Relative expression level
VCAM-1 35-45kD
VCAM-1 85-100kD
ICAM-1
C
control 0.25μM 0.5μM
HDAC 6
Ace-tubulin
ERK
p-ERK
β-actin
D
control
0.25μm
0.5μm
Relative expression level
HDAC6
Ace-tubulin
p-ERK/ERK
E
control 0.25μM 0.5μM
p-AKT
AKT
β-actin
F
control
0.25μM
0.5μM
Relative expression level
p-AKT/t-AKT
G
control
control +u0126
0.5μM +u0126
ERK
p-ERK
Ace-tubulin
β-actin
H
control
control+u0126
0.5μM+u0126
Relative expression level
Ace-tubulin
p-ERK/ERK
I
control
Control +u0126
0.5μM +u0126
VCAM-1
35-45 kD
VCAM-1
85-100 kD
ICAM-1
β-actin
J
control
control+u0126
0.5μM+u0126
Relative expression level
VCAM-1 35-45kD
VCAM-1 85-100kD
ICAM-1

Figure 5. Protein expression levels in cells of each group. A. The effects of 0.25 μM and 0.5 μM tubacin on VCAM-1 (35-45 kDa), VCAM-1 (85-100 kDa), and ICAM. B. Western blot results were analyzed by Image-Pro Plus 6. *P < 0.05 compared with the control group; **P < 0.01 compared with the control group. C. The effects of 0.25 μM and 0.5 μM tubacin on HDAC6, acetylated α-tubulin (ace-tubulin), ERK, and p-ERK. D. Western blot results were analyzed by Image-Pro Plus 6. *P < 0.05 compared with the control group; **P < 0.01 compared with the control group. E. The effects of 0.25 μM and 0.5 μM tubacin on p-Akt. F. Western blot results were analyzed by Image-Pro Plus 6. Data are presented as mean ± SD. *P < 0.05 compared with the control group. G. The effects of U0126 and 0.5 μM tubacin+U0126 on HDAC6, ace-tubulin, ERK, and p-ERK. H. Western blot results were analyzed by Image-Pro Plus 6. *P < 0.05 compared with the control+U0126 group. **P < 0.01 compared with the control+U0126 group. I. The effects of U0126 and 0.5 μM tubacin+U0126 on VCAM-1 (35-45 kDa), VCAM-1 (85-100 kDa), and ICAM-1. J. Western blot results were analyzed by Image-Pro Plus 6. *P < 0.05 compared with the control+U0126 group; **P < 0.01 compared with the control group; #P < 0.01 compared with the control+U0126 group. U0126 is an ERK pathway inhibitor. Data are presented as mean ± SD. Comparisons were performed by one-way analysis of variance (ANOVA) among groups or by Student's t test between two groups.

BMSCs were plated at 2 × 10^5 cells/ml in a 35-mm culture dish. After 30 min, the culture medium was aspirated and the cells were washed twice with PBS. Hoechst 33258 staining solution was added to the dish, and the cells were cultured at 37°C with 5% CO_2 for 20 min. The staining solution was discarded, and the dish was washed three times with DMEM/F12 medium. The dish was observed with a fluorescence microscope. Ten locations were selected randomly and the number of cells was recorded.

Western blot detection of protein expression levels

The BMSCs were plated into 6-well plates at a density of 4 × 10^4 cells/well. The cells were pretreated with different concentrations of tubacin for 24 h. Harvested cells were lysed by incubation in RIPA buffer with Protease Inhibitor Cocktail for 30 min at 4°C. Lysates were centrifuged for 15 min at 12,000 × *g* at 4°C. Then the supernatants were collected and frozen at -80°C or used immediately. Total protein was extracted and separated by SDS-PAGE. The proteins were transferred to the membranes, which were incubated with primary and secondary antibodies, and a reagent was added for band visualization. VCAM-1 (35-45 kDa), VCAM-1 (85-100 kDa), ICAM, α-tubulin, acetylated α-tubulin (ace-α-tubulin), ERK, p-ERK, Akt and Phospho-Akt were detected. Western blot results were analyzed by Image-Pro Plus 6.

Ray Biotech protein chip analysis

In each group, 10^7 cells were taken. After washing with PBS, a total protein extraction reagent (1 ml) containing protease inhibitor was added to the cells. The protein concentration was determined by BCA assay. The antibody chip was incubated in buffer for 30 minutes and then incubated with protein sample at room temperature for 2 h. The chip was washed with washing buffer, a biotin-labeled antibody was added, and the chip was incubated at room temperature for 2 h. After thoroughly cleaning with washing buffer, the chemiluminescent reagent was added and the film was exposed. Finally, the film was scanned and a digital image was obtained. The protein signal intensity was quantified by the gray value, which was normalized with the control sample. Differentially expressed proteins were obtained by comparison of normalized values between groups.

Data processing and statistical analysis

All of the experiments were repeated at least three times. All of the data were statistically analyzed by SPSS 19 software. The related digital variables are expressed as mean ± SD. Comparisons were performed by one-way analysis of variance (ANOVA) among groups or by Student's *t* test between two groups. If P < 0.05 the result was considered to be statistically significant.

Results

Effect of low tubacin concentration on proliferation and adhesion of BMSCs

Cultured BMSCs reached a confluecy of 80-90% at about 5 days (**Figure 1A**) or 6 days (**Figure 1B**). After two passages, the cells were arranged in a radial or swirling way, and the morphology was the same (**Figure 1C**, **1D**). Compared with the control group, cell viability was significantly increased in the tubacin treatment groups and

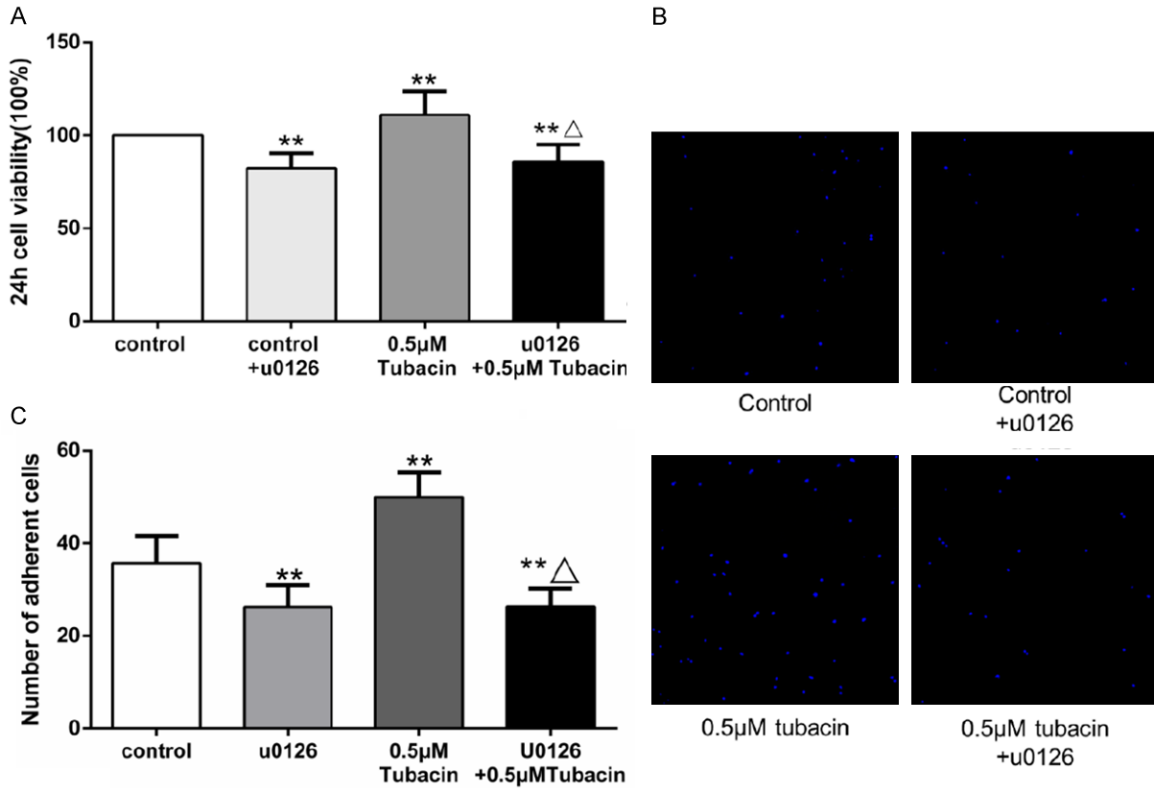

Figure 6. Inhibition of ERK signaling pathways reduces tubacin-induced proliferation and adhesion of BMSCs. A. BMSCs were treated with tubacin 0.5 μM for 24 h in combination with U0126 10 μM. Cell viability was assessed by MTT assay. B, C. Cell adhesion were analyzed by Hoechst 33258 staining. Data are presented as mean ± SD. $^{**}P < 0.01$ compared with the control group; $\Delta P < 0.01$ compared with the 0.5 μM Tubacin group.

it peaked at a tubacin concentration of 0.5 μM (**Figure 1E**). With increasing tubacin concentrations, the number of adherent cells also increased significantly ($P < 0.05$) (**Figure 1F**, **1G**). Therefore, tubacin concentrations of 0.25 μM and 0.5 μM were selected for subsequent experiments. These results show that a low concentration of tubacin could promote BMSC adhesion and proliferation.

Effect of low tubacin concentration on migration of BMSCs

Results of the wound scratching assay are shown in **Figure 2**. At the same time point, tubacin promoted more BMSCs to migrate across the wound edge into the scratch area than in the control group. Transwell chambers were also used to determine the effect of tubacin on BMSC migration. Compared with the control group, more cells were stained blue after tubacin treatment, and the number of invasive cells was considerably higher than in the control group. The difference was statistically significant ($P < 0.01$).

The surface morphology, ultrastructure, and cell stiffness of BMSCs are correlated with the concentration of tubacin

To observe the effect of tubacin on morphological and surface ultrastructural changes in BMSCs, high-resolution atomic force microscopy (AFM) was used. Under control conditions, BMSCs are mainly spindle-shaped and the filopodia form a connecting mesh between adjacent cells. **Figure 3A** and **3B** show the membrane surface ultrastructure of BMSCs at 5 μm × 5 μm. It is obvious that normal BMSCs were rough and uneven, there were clear holes and sags on the cell membrane, and the surface particles were not evenly distributed. With increasing tubacin concentrations, the surface of the cells was smoother and the distribution of particles was more uniform. AFM can not only provide important detailed information

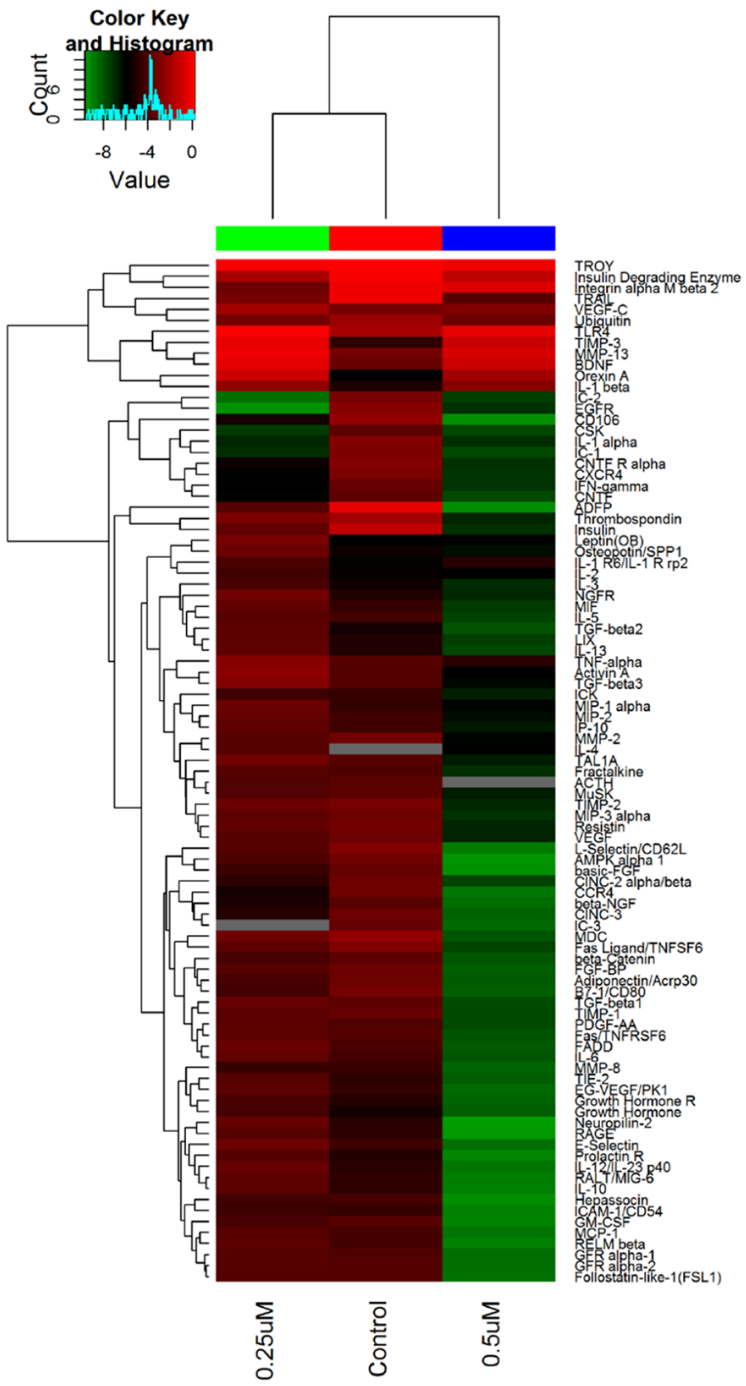

Figure 7. Heat map of protein chip clustering analysis. BMSCs were divided into three groups: untreated control cells, 0.25 μM tubacin group, and 0.5 μM tubacin group. The effects of tubacin on intracellular protein expression, as determined by protein chip analysis, are shown.

about cell morphology, but also quantify a large amount of specific data on the cell structure. With increasing tubacin concentrations, cells became more elongated and had longer and richer pseudopodia. Upon treatment with 0.25 and 0.5 μM tubacin, the length of BMSCs increased rapidly from 43.7 μm to 70.4 μm and 81.4 μm, respectively; the height increased remarkably from 20-100 nm to 50-200 nm and 80-200 nm, respectively (**Figure 3C**, **3D**).

The results show that the root mean square roughness (Rq) and the average roughness (Ra) of the cell membrane surface in the tubacin treatment group were significantly lower than those of the control group (**Figure 4E**; **Table 1**).

Using AFM we were able to measure the force-distance curve and analyze the mechanical properties of the cell membrane. Yang's modulus reflects the rigidity of the surface of the cell membrane. With increasing tubacin concentrations, Young's modulus gradually increased, indicating that the cytoskeleton was more tightly arranged and the ability to resist deformation and mechanical stress was enhanced after tubacin treatment (**Figure 4D**).

Western blot detection of VCAM-1, ICAM-1, HDAC6, p-ERK, p-Akt and acetylated α-tubulin

α-Tubulin, which is expressed at relatively stable levels in different cells, is an important substrate molecule of HDAC6. Tubacin can upregulate the protein levels of VCAM-1, ICAM-1, p-ERK, and acetylated α-tubulin, which could be inhibited by the ERK pathway inhibitor U0126. Furthermore, tubacin can downregulate the protein levels of p-Akt (**Figure 5**). These results suggest that HDAC6 inhibitors may be involved in the acetylation of α-tubulin through the ERK pathway.

Table 2. Upregulated cytokines after tubacin treatment

	Cytokine	Control group	Tubacin group	Fold change
1	Activin A	0.06551	0.16767	2.56
2	BDNF	0.09594	0.71200	7.42
3	E-Selectin	0.04812	0.10337	2.15
4	Growth hormone	0.02510	0.05421	2.16
5	IL-1 β	0.02873	0.18459	6.42
6	IL-1 R6/IL-1 R	0.01472	0.06242	4.24
7	IL-2	0.01952	0.04957	2.54
8	IL-3	0.02212	0.05816	2.63
9	IL-10	0.03806	0.07879	2.07
10	IL-12/IL-23 p40	0.03464	0.09256	2.67
11	IL-13	0.02975	0.08361	2.81
12	Leptin (OB)	0.01612	0.12123	7.52
13	LIX	0.03101	0.07771	2.51
14	MIF	0.04099	0.08811	2.15
15	MIP-1α	0.03914	0.10151	2.59
16	MMP-13	0.11368	0.85858	7.55
17	Neuropilin-2	0.03280	0.09351	2.85
18	NGFR	0.03087	0.11390	3.69
19	Orexin A	0.01785	0.50598	28.35
20	Osteopotin/SPP1	0.02187	0.09865	4.51
21	Prolactin R	0.03014	0.06715	2.23
22	RALT/MIG-6	0.03724	0.07891	2.12
23	TGF-β2	0.02404	0.07713	3.21
24	TGF-β3	0.06754	0.14740	2.18
25	TIMP-3	0.03757	0.80961	21.55
26	TLR4	0.27112	1.06822	3.94
27	TNF-α	0.06943	0.15684	2.26
28	VEGF-C	0.12025	0.24668	2.05

The effect of U0126, ERK pathway inhibitor, on BMSCs proliferation and adhesion

To determine whether the effect of tubacin on the proliferation of BMSCs depends on ERK signaling pathways, BMSCs were pre-treated with the inhibitors U0126 (10 μmol/L). Cell viability of the tubacin-treated group was significantly higher than that of the tubacin group pre-treated with U0126 and the control group at 24 hours. $^{**}P < 0.01$ compared with the control group, $\Delta P < 0.01$ compared with the 0.5 μM Tubacin group (**Figure 6A**). The adhesion assay also showed that the BMSCs proliferation ratio increased significantly by tubacin treatment compared to the control group and this increase was blocked by the pre-treatment with U0126 ($^{**}P < 0.01$ compared with the control group, $\Delta P<0.01$ compared with the 0.5 μM Tubacin group, **Figure 6B**, **6C**). These results demonstrate that the ERK Signaling pathway is involved in the promotive effect of tubacin on BMSCs proliferation and adhesion.

Ray Biotech protein chip analysis of cytokines

The raw Ray Biotech protein chip data were corrected by subtracting the minimum value and normalized by Pos. The signal value ratio method is used for analysis. We considered signal values greater than 500 and fold change values greater than 2 (or less than 0.5). After tubacin treatment, there were significant changes in the expression levels of 49 cytokines, including (i) brain-derived neurotrophic factor (BDNF) and its receptor (NGFR) and (ii) interleukins (ILs) and their receptors. These interleukins play roles in inflammatory responses and the regulation of immune cells by stimulating cell activation, proliferation, and differentiation (**Figures 6** and **7**; **Tables 2** and **3**).

Discussion

In recent years, many studies have confirmed that HDACs play an important role in cell proliferation and differentiation [18, 19]. HDAC6 is a unique member of the HDAC family, and it can specifically catalyze histone and non-histone substrates. Tubacin is a highly potent and selective, reversible cell-permeable inhibitor of HDAC6 by chelating a Zn^{2+} cation in the catalytic pocket [20].

HDAC6 participates in the regulation of cell movement by interacting with its substrate proteins, which include α-tubulin, cortactin, and HSP90 [21]. However, the function of HDAC6 in stem cell proliferation and migration remains largely unknown.

The morphology and ultrastructure of the cells are closely related to the physiological state and function of the cells. All kinds of biological macromolecules which are localized in the cell membrane, such as carbohydrates, proteins, and lipids, not only maintain the integrity of the

Table 3. Downregulated cytokines after tubacin treatment

	Cytokine	Control group	Tubacin group	Fold change
1	ADFP	0.81129	0.06959	0.09
2	B7-1/CD80	0.11892	0.05142	0.43
3	β-FGF	0.09006	0.04431	0.49
4	β-NGF	0.07320	0.02717	0.37
5	CCR4	0.10647	0.02480	0.23
6	CD106	0.19023	0.02382	0.13
7	CINC-2 α/β	0.10283	0.03609	0.35
8	CINC-3	0.10260	0.03315	0.32
9	CNTF	0.07862	0.01477	0.19
10	CNTF Rα	0.14365	0.02205	0.15
11	CSK	0.07754	0.00634	0.08
12	CXCR4	0.13309	0.01668	0.13
13	EGFR	0.15862	0.00147	0.01
14	IC-2	0.12428	0.00266	0.02
15	IC-1	0.13691	0.00781	0.06
16	IDE	1.03220	0.27034	0.26
17	IFN-γ	0.09150	0.01759	0.19
18	IL-1α	0.14478	0.00890	0.06
19	IntegrinαMβ2	0.87307	0.10138	0.12
20	Insulin	0.39290	0.08419	0.21
21	TRAIL	0.92022	0.12297	0.13

cell membrane, but also transmit cellular signals, which are involved in the regulation of cell proliferation, differentiation, migration, and intercellular interaction [22-24]. In this study, BMSCs treated by tubacin extended into a long fusiform shape and exhibited more pseudopodia, which not only facilitated the transmission of information between cells but also increased the contact area between cells and substrate. The surface roughness of the membrane is also an important parameter of the cell ultrastructure, which is related to the integrity of the cytoskeleton [25]. In this study, the surface grain size of tubacin-treated cells increased and the roughness decreased, which may be a result of the interaction of macromolecules on the surface of the cell membrane with the rearranged intracellular skeleton.

Cell hardness can directly reflect the formation of cytoskeleton, and the inner skeleton of cells with higher hardness is more tightly arranged, can bear a higher external force, and can maintain the cellular structure during migration [26]. AFM mechanical tests showed that Young's modulus of BMSCs was greater after tubacin treatment, possibly due to a more powerful driving force for stretching and retraction during cell movement, which also helps to maintain movement direction and enhances the cell's migration ability.

Furthermore, cell migration heavily depends on the ability and speed of cell-matrix adhesion and release. Intercellular adhesion molecule 1 (ICAM-1) and vascular cell adhesion molecule 1 (VCAM-1) belong to the immunoglobulin superfamily, which mediate the adhesion of neutrophils and mononuclear cells to vascular endothelial cells, activate lymphocytes, and promote the migration of leukocytes to inflammatory areas [27, 28]. VCAM-1 is also involved in the regulation of the migration and homing of stem cells [29, 30]. Our study shows that the protein expression levels of VCAM-1 and ICAM-1 were significantly increased after tubacin treatment, which could be suppressed by the ERK inhibitor U0126.

Conclusion

In conclusion, pretreatment of BMSCs with a low concentration of tubacin can improve the morphology and mechanical properties of BMSCs, which could enhance the cells' migration ability and protect them from pathological damage.

Furthermore, a low tubacin concentration could promote the proliferation of BMSCs, increase the levels of VCAM-1, ICAM-1, acetylated α-tubulin, and p-ERK, thus promoting the adhesion and migration ability of BMSCs. Our findings suggest that the protective effects of tubacin on BMSCs likely involve the inhibition of HDAC6 by activation of the ERK pathway.

Acknowledgements

The authors gratefully acknowledge the financial support of Science & Technology Planning Project of Dongguan & Guangdong Province, China (No: 2015A020214020, 4SG17039G, 2017507152431). This research is part of the Guangdong Medical Science and Technology Research Fund Project (No: B2018032).

Disclosure of conflict of interest

None.

Address correspondence to: Dr. Xin-Sheng Peng, Institute of Marine Medicine, Guangdong Medical University, Dongguan 523808, China. Tel: +86-13556715510; E-mail: gdmcpxs@163.com; Dr. Yan-Fang Zhou, Department of Pathophysiology, Guangdong Medical University, Dongguan 523808, China. Tel: +86-13827299246; E-mail: yfzhou@gdmu.edu.cn

References

[1] Zhang Y, Huang X and Yuan Y. MicroRNA-410 promotes chondrogenic differentiation of human bone marrow mesenchymal stem cells through down-regulating Wnt3a. Am J Transl Res 2017; 9: 136-145.

[2] Li Y, Chen J, Chen XG, Wang L, Gautam SC, Xu YX, Katakowski M, Zhang LJ, Lu M, Janakiraman N and Chopp M. Human marrow stromal cell therapy for stroke in rat: neurotrophins and functional recovery. Neurology 2002; 59: 514-523.

[3] Chen J, Li Y, Wang L, Zhang Z, Lu D, Lu M and Chopp M. Therapeutic benefit of intravenous administration of bone marrow stromal cells after cerebral ischemia in rats. Stroke 2001; 32: 1005-1011.

[4] Chen T, Zhu H, Wang Y, Zhao P, Chen J, Sun J, Zhang X and Zhu G. Apoptosis of bone marrow mesenchymal stromal/stem cells via the MAPK and endoplasmic reticulum stress signaling pathways. Am J Transl Res 2018; 10: 2555-2566.

[5] Lv B, Hua T, Li F, Han J, Fang J, Xu L, Sun C, Zhang Z, Feng Z and Jiang X. Hypoxia-inducible factor 1 alpha protects mesenchymal stem cells against oxygen-glucose deprivation-induced injury via autophagy induction and PI3K/AKT/mTOR signaling pathway. Am J Transl Res 2017; 9: 2492-2499.

[6] Kaluza D, Kroll J, Gesierich S, Yao TP, Boon RA, Hergenreider E, Tjwa M, Rossig L, Seto E, Augustin HG, Zeiher AM, Dimmeler S and Urbich C. Class IIb HDAC6 regulates endothelial cell migration and angiogenesis by deacetylation of cortactin. EMBO J 2011; 30: 4142-4156.

[7] Williams KA, Zhang M, Xiang S, Hu C, Wu JY, Zhang S, Ryan M, Cox AD, Der CJ, Fang B, Koomen J, Haura E, Bepler G, Nicosia SV, Matthias P, Wang C, Bai W and Zhang X. Extracellular signal-regulated kinase (ERK) phosphorylates histone deacetylase 6 (HDAC6) at serine 1035 to stimulate cell migration. J Biol Chem 2013; 288: 33156-33170.

[8] Park SY, Phorl S, Jung S, Sovannarith K, Lee SI, Noh S, Han M, Naskar R, Kim JY, Choi YJ and Lee JY. HDAC6 deficiency induces apoptosis in mesenchymal stem cells through p53 K120 acetylation. Biochem Biophys Res Commun 2017; 494: 51-56.

[9] Tsai MJ, Tsai SK, Hu BR, Liou DY, Huang SL, Huang MC, Huang WC, Cheng H and Huang SS. Recovery of neurological function of ischemic stroke by application of conditioned medium of bone marrow mesenchymal stem cells derived from normal and cerebral ischemia rats. J Biomed Sci 2014; 21: 5.

[10] Bang OY, Lee JS, Lee PH and Lee G. Autologous mesenchymal stem cell transplantation in stroke patients. Ann Neurol 2005; 57: 874-882.

[11] Pavlichenko N, Sokolova I, Vijde S, Shvedova E, Alexandrov G, Krouglyakov P, Fedotova O, Gilerovich EG, Polyntsev DG and Otellin VA. Mesenchymal stem cells transplantation could be beneficial for treatment of experimental ischemic stroke in rats. Brain Res 2008; 1233: 203-213.

[12] Parr AM, Tator CH and Keating A. Bone marrow-derived mesenchymal stromal cells for the repair of central nervous system injury. Bone Marrow Transplant 2007; 40: 609-619.

[13] Hong SQ, Zhang HT, You J, Zhang MY, Cai YQ, Jiang XD and Xu RX. Comparison of transdifferentiated and untransdifferentiated human umbilical mesenchymal stem cells in rats after traumatic brain injury. Neurochem Res 2011; 36: 2391-2400.

[14] Lee JB, Kuroda S, Shichinohe H, Yano S, Kobayashi H, Hida K and Iwasaki Y. A pre-clinical assessment model of rat autogeneic bone marrow stromal cell transplantation into the central nervous system. Brain Res Brain Res Protoc 2004; 14: 37-44.

[15] Wang B, Zhu X, Kim Y, Li J, Huang S, Saleem S, Li RC, Xu Y, Dore S and Cao W. Histone deacetylase inhibition activates transcription factor Nrf2 and protects against cerebral ischemic damage. Free Radic Biol Med 2012; 52: 928-936.

[16] Selvi BR, Cassel JC, Kundu TK and Boutillier AL. Tuning acetylation levels with HAT activators: therapeutic strategy in neurodegenerative diseases. Biochim Biophys Acta 2010; 1799: 840-853.

[17] Wang Z, Leng Y, Wang J, Liao HM, Bergman J, Leeds P, Kozikowski A and Chuang DM. Tubastatin A, an HDAC6 inhibitor, alleviates stroke-induced brain infarction and functional deficits: potential roles of alpha-tubulin acetylation and FGF-21 up-regulation. Sci Rep 2016; 6: 19626.

[18] Sun JY, Wang JD, Wang X, Liu HC, Zhang MM, Liu YC, Zhang CH, Su Y, Shen YY, Guo YW, Shen AJ and Geng MY. Marine-derived chromopeptide A, a novel class I HDAC inhibitor, suppresses human prostate cancer cell proliferation

and migration. Acta Pharmacol Sin 2017; 38: 551-560.
[19] Li A, Liu Z, Li M, Zhou S, Xu Y, Xiao Y and Yang W. HDAC5, a potential therapeutic target and prognostic biomarker, promotes proliferation, invasion and migration in human breast cancer. Oncotarget 2016; 7: 37966-37978.
[20] Aldana-Masangkay GI and Sakamoto KM. The role of HDAC6 in cancer. J Biomed Biotechnol 2011; 2011: 875824.
[21] Ran J, Yang Y, Li D, Liu M and Zhou J. Deacetylation of alpha-tubulin and cortactin is required for HDAC6 to trigger ciliary disassembly. Sci Rep 2015; 5: 12917.
[22] Tang BL. Rab, Arf, and Arl-regulated membrane traffic in cortical neuron migration. J Cell Physiol 2016; 231: 1417-1423.
[23] Lanier MH, McConnell P and Cooper JA. Cell migration and invadopodia formation require a membrane-binding domain of CARMIL2. J Biol Chem 2016; 291: 1076-1091.
[24] Gauvin TJ, Young LE and Higgs HN. The formin FMNL3 assembles plasma membrane protrusions that participate in cell-cell adhesion. Mol Biol Cell 2015; 26: 467-477.
[25] Wang Y, Xu C, Jiang N, Zheng L, Zeng J, Qiu C, Yang H and Xie S. Quantitative analysis of the cell-surface roughness and viscoelasticity for breast cancer cells discrimination using atomic force microscopy. Scanning 2016; 38: 558-563.
[26] Schaefer A and Hordijk PL. Cell-stiffness-induced mechanosignaling - a key driver of leukocyte transendothelial migration. J Cell Sci 2015; 128: 2221-2230.
[27] Lee S, Yoon IH, Yoon A, Cook-Mills JM, Park CG and Chung J. An antibody to the sixth Ig-like domain of VCAM-1 inhibits leukocyte transendothelial migration without affecting adhesion. J Immunol 2012; 189: 4592-4601.
[28] Lyck R and Enzmann G. The physiological roles of ICAM-1 and ICAM-2 in neutrophil migration into tissues. Curr Opin Hematol 2015; 22: 53-59.
[29] Perdomo-Arciniegas AM and Vernot JP. Co-culture of hematopoietic stem cells with mesenchymal stem cells increases VCAM-1-dependent migration of primitive hematopoietic stem cells. Int J Hematol 2011; 94: 525-532.
[30] Nishihira S, Okubo N, Takahashi N, Ishisaki A, Sugiyama Y and Chosa N. High-cell density-induced VCAM1 expression inhibits the migratory ability of mesenchymal stem cells. Cell Biol Int 2011; 35: 475-481.